Kobe J. Med. Sci., Vol. 62, No. 5, pp. E136-E141, 2016

Increased Pittsburgh Compound-B Accumulation in the Subcortical White Matter of Alzheimer's Disease Brain

YUICHI WAKABAYASHI[1], KAZUNARI ISHII[2], CHISA HOSOKAWA[2], TOMOKO HYODO[2], HAYATO KAIDA[2], MINORU YAMADA[2], YUKINOBU YAGYU[2], MASAKATSU TSURUSAKI[2], TAKENORI KOZUKA[2], KAZURO SUGIMURA[1] and TAKAMICHI MURAKAMI[2]

[1] Department of Radiology, Kobe University Graduate School of Medicine, Kobe, Hyogo, Japan

[2] Department of Radiology, Kindai University Faculty of Medicine, Osakasayama, Osaka, Japan

Received 24 October 2016/ Accepted 19 December 2016

Keywords: Dementia, Alzheimer's disease, ^{11}C-PiB-PET, White matter, Amyloid deposit

Using ^{11}C-Pittsburgh compound B (PiB)-PET and MRI volume data, we investigated whether white matter (WM) PiB uptake in Alzheimer's disease (AD) brain is larger than that of cortical PiB uptake-negative (PiB-negative) brain. Forty-five subjects who underwent both PiB-PET and MRI were included in the study (32 AD patients with cortical PiB-positive and 13 cortical amyloid -negative patients). Individual areas of gray matter (GM) and WM were segmented, then regional GM and WM standard uptake value ratio (SUVR) normalized to cerebellar GM with partial volume effects correction was calculated. Three regional SUVRs except WM in the centrum semiovale in the AD group were significantly larger than those in the PiB-negative groups. Frontal WM SUVR in the AD group vs frontal WM SUVR in the PiB-negative group was 2.57 ± 0.55 vs 1.64 ± 0.22; parietal, 2.50 ± 0.52 vs 1.74 ± 0.22; posterior cingulate, 2.84 ± 0.59 vs 1.73 ± 0.22; and WM in the centrum semiovale, 2.21 ± 0.53 vs 2.42 ± 0.36, respectively. We found that PiB uptake in AD brain is significantly larger than that in PiB-negative brain in the frontal, parietal and posterior cingulate subcortical WM, except in the centrum semiovale.

INTRODUCTION

Alzheimer disease (AD) is the most common neurodegenerative disease and a leading cause of dementia (1). The hallmarks of AD pathology are the formation of amyloid beta (Aβ) plaques and the aggregation of tau protein into neurofibrillary tangles (2). ^{11}C-Pittsburgh compound B (PiB) positron emission tomography (PET) is considered to be a useful method for evaluating AD. PiB retention in the cortex is typically used to distinguish between individuals with cognitive problems who have AD-type pathology and those who do not, or to predict which cognitively normal or mildly impaired persons might develop cognitive decline in the future (3, 4). PiB is similarly retained in the white matter (WM) of healthy individuals and in brains of AD patients, but the specificity of PiB retention in the WM is unclear. Recently, in addition to gray matter (GM) pathology, WM changes were recognized as an important pathological feature in the emergence of AD (5, 6). In our clinical setting, we speculated that PiB retention in WM of AD patients is significantly larger than in WM of PiB retention-negative patients. In this study, we evaluated regional WM PiB retentions in AD patients and PiB retention-negative patients. Using PiB-PET and magnetic resonance imaging (MRI) volume data, we investigated whether WM PiB uptake in AD brain is larger than that in PiB retention-negative brain.

MATERIALS AND METHODS

Subjects

This study was approved by the institutional review board and the requirement for informed consent was waved. Forty-five subjects who complained of cognitive impairments and underwent both PiB-PET and MRI were included in this study (32 AD patients with PiB-positive accumulation, mean age 70.1 ± 8.0 years, male to female ratio = 17:15, Mini Mental State Examination (MMSE) 19.0 ± 4.8; and 13 subjects with PiB-negative accumulation, mean age 66.5 ± 7.0 years, male to female ratio = 7:6, MMSE 28.2 ± 1.4) (Table I). All patients were examined by routine laboratory tests, structural neuroimaging (PiB-PET and MRI), and standard neuropsychological examinations, including the MMSE. The AD patients fulfilled National Institute of Neurological and Communicative Disorders and Stroke and the Alzheimer's Disease and Related Disorders Association criteria (7). For the PiB-negative accumulation group we selected subjects with subjective cognitive impairment without AD

Phone: +81-78-382-6104 Fax: +81-78-382-6129 E-mail:baya318@yahoo.co.jp

and other dementia clinically. We excluded cognitive impairment subjects with MMSE score under 25. PiB-PET images of all subjects were visually assessed by two experienced nuclear medicine physicians blinded to the clinical information separately. If two visual ratings were not consistent, consensus was achieved by discussion. PiB positivity was evaluated in cortical regions, including the bilateral frontal lobes, parietotemporal lobes, occipital lobes, precuneus/posterior cingulate gyri and striata. According to the PiB positivity in each region, each subject was classified as PiB-positive or PiB-negative. For each region, PiB-positive was defined as higher accumulation in the cerebral cortex than in the WM, and PiB-negative was defined as no cortical accumulation.

Table I. Demographic and clinical characteristics of the PiB-negative and AD groups.

	PiB-negative	AD
Number of subjects	13	32
Male: Female	7: 6	17: 15
Age (years)	66.5 ± 7.0	70.1 ± 8.0
MMSE	28.2 ± 1.4	19.0 ± 4.8

PiB = ^{11}C-Pittsburgh compound B; AD = Alzheimer's disease; MMSE = Mini Mental State Examination. Data are mean ± SD.

PiB-PET

^{11}C-PiB was synthesized at our institution's PET facility, as described previously (8). PET scans were performed using a PET scanner (ECAT Accel, Siemens AG, Erlangen, Germany) in the 3D mode. A transmission scan was performed for correction of attenuation before administration of the tracer. ^{11}C-PiB was injected into an antecubital vein, at a mean dose of 555 ± 185 MBq (11.1 MBq/kg body weight), and then the vein was flushed with saline. Images were acquired 50–70 min after injection. The images were reconstructed with an iterative algorithm that provided spatial and axial resolution in the range of 6–8 mm at full-width and half-maximum. For visual inspection, standard uptake value images were obtained with a rainbow color scale by normalizing the tissue radioactivity.

MRI

All subjects underwent repeated structural MRI scans using a 3T Achieva scanner (Philips, Amsterdam, Netherlands). The scan protocol included a coronal T1-weighted three dimensional magnetization prepared rapid acquisition gradient echo sequence (slice thickness 1.2 mm, 170 slices, matrix size 256 × 256, voxel size 1 × 1 × 1 mm, echo time 3.1 ms, repetition time 6.7 ms, flip angle 8°) and was used for co-registration, segmentation and definition of voxels of interest (VOI).

Image Analysis

For image analysis, automatic volumetric measurement of segmented brain images system (AVSIS) software was used (9). In brief, before this analysis, VOI templates for the frontal, parietal, posterior cingulate, centrum semiovale and cerebellar cortices were prepared (Fig. 1). Each regional VOI template was produced on a digital phantom: the Simulated Brain Database (http://www.bic.mni.mcgill.ca/brainweb/) in standard Montreal Neurological Institute space (10), manually delineating the contours of each structure. The process of modified AVSIS is as follows: first, each individual MR image and PiB-PET image were co-registered, and then each subject's MR image was segmented into GM, WM, and cerebrospinal fluid with the Statistical Parametric Mapping-8 segmentation program (Wellcome Trust Centre for Neuroimaging, London, United Kingdom) in MATLAB 2009B (The MathWorks Inc., Natick, MA, USA) (11-13). The GM template image derived from the Simulated Brain Database was then spatially transformed into the individual subject's GM image, and a normalization parameter produced Diffeomorphic Anatomical Registration Through Exponentiated Lie Algebra algorithm (14). Using this parameter, the frontal, parietal, posterior cingulate, centrum semiovale and cerebellum VOI templates were transformed to the individual subject's space. Then, partial volume effects corrected PiB-PET images were created using previously described techniques (15). Next, the frontal, parietal, posterior cingulate, centrum semiovale and cerebellar PiB uptake counts on GM and WM were separately calculated by determining the regions of co-registered partial volume effects corrected PiB images on each extracted area using the described volumetric procedure (Fig. 2), and finally, regional GM and WM Standard Uptake Value Ratio (SUVR) normalized to cerebellar GM was calculated. The regional SUVRs were analyzed by repeated measures analysis of variance with one between-subject factor (AD or PiB-negative group) and two within-subject factors (location

(the frontal, parietal, posterior cingulate or centrum semiovale) and WM/GM nested in location). Because of the specific hypothesis, planned multiple comparisons were performed between the two groups as a function of the location using Scheffe test. The level of significance was set at $P < 0.05$.

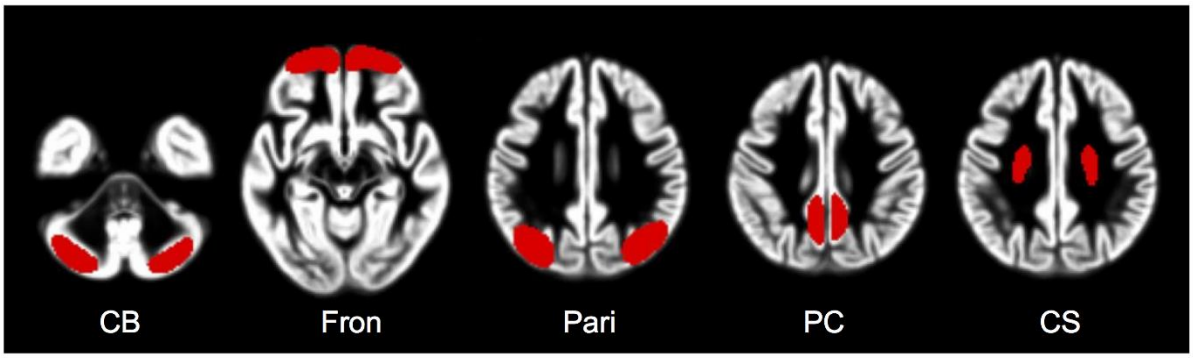

Figure 1. VOI template of five regions. CB = cerebellum, Fron = frontal, Pari = parietal, PC = posterior cingulate, CS = centrum semiovale.

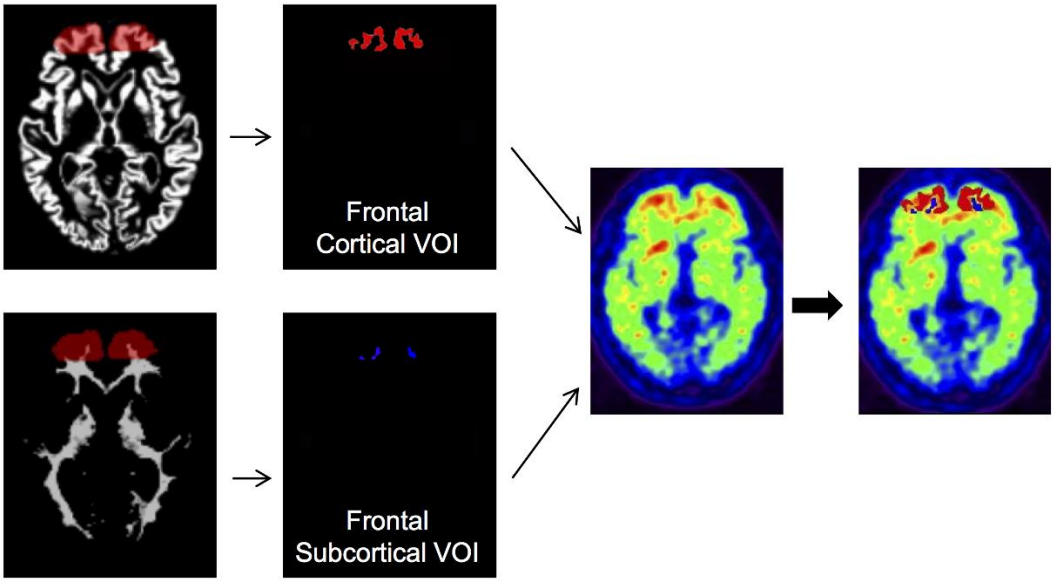

Figure 2. Algorithm for calculating frontal GM and WM amyloid depositions. Individual GM and WM images were segmented, then cortical and subcortical VOIs were created from the transformed frontal VOI. Frontal cortical and subcortical WM PiB counts were measured on the co-registered individual PiB image using these VOIs.

RESULTS

Three regional SUVRs, except WM in the centrum semiovale in the AD group, were significantly larger than those in the PiB-negative group ($P < 0.05$). Frontal WM SUVR in the AD group vs frontal WM SUVR in the PiB-negative group was 2.57 ± 0.55 vs 1.64 ± 0.22; parietal, 2.50 ± 0.52 vs 1.74 ± 0.22; posterior cingulate, 2.84 ± 0.59 vs 1.73 ± 0.22; and WM in the centrum semiovale, 2.21 ± 0.53 vs 2.42 ± 0.36, respectively. In addition to WM SUVR, we analyzed cortical SUVR in each area. Frontal cortical SUVR in the AD group vs frontal cortical SUVR in the PiB-negative group was 3.72 ± 1.02 vs 1.16 ± 0.15; parietal, 3.71 ± 0.83 vs 1.16 ± 0.22; posterior cingulate, 4.54 ±0.99 vs 1.25 ± 0.20, respectively (Fig. 3).

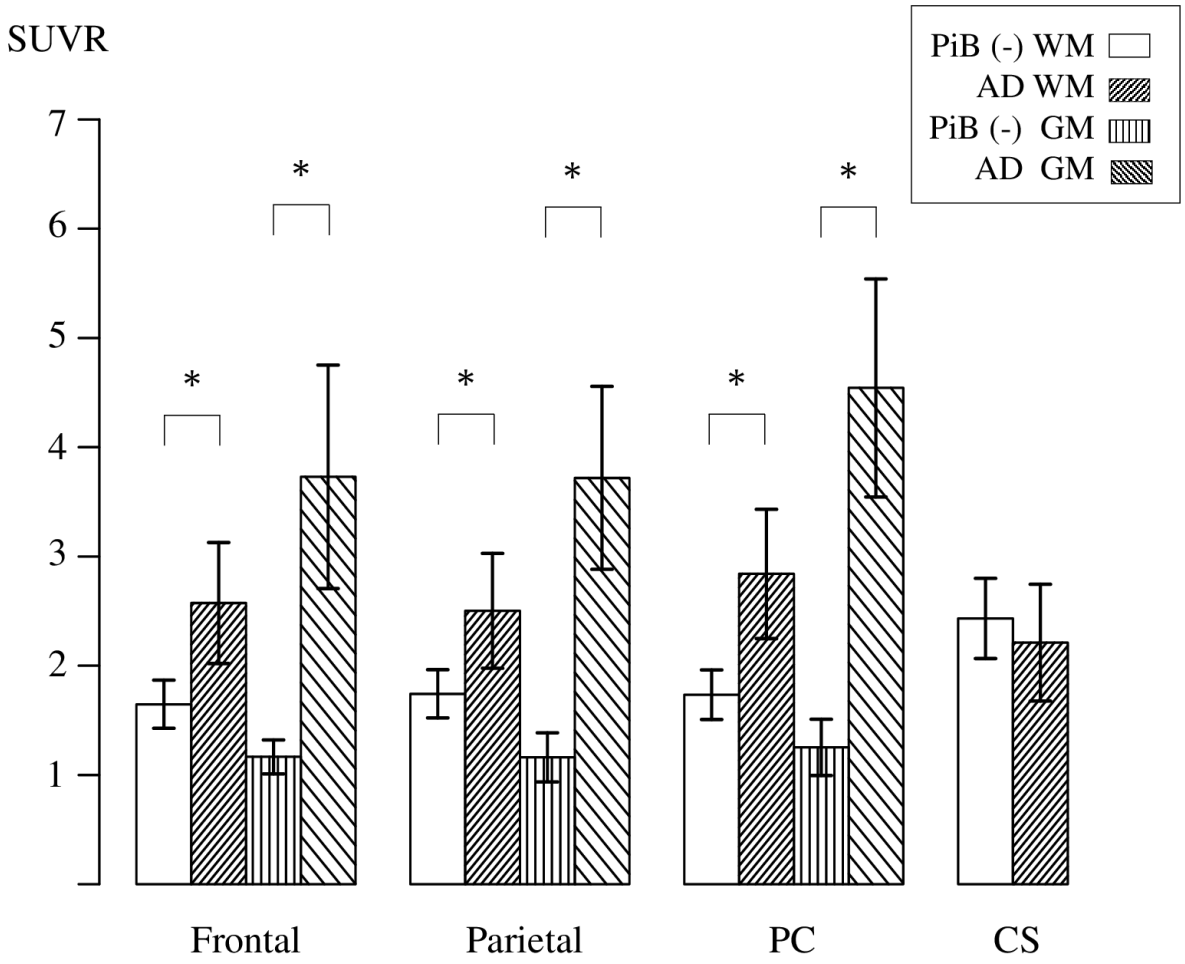

Figure 3. Regional SUVRs in AD and PiB-negative groups. Subcortical WM PiB uptake in the frontal, parietal and posterior cingulate regions of the AD group was significantly greater than the PiB-negative group. PC = posterior cingulate; CS = centrum semiovale; WM = white matter; GM = gray matter; PiB (−) = PiB-negative. *P < 0.05.

DISCUSSION

In this study, we found that frontal, parietal and posterior cingulate WM SUVRs in the AD group were significantly greater than those in the PiB-negative groups. PiB retention in the WM has been reported to be non-specific, and the degree of PiB accumulation was shown to be equal between the AD group and healthy controls (2, 16). In addition, the accumulation of PiB in the subcortical WM is believed to spill over due to the accumulation of PiB in the cortex. Compared with previous studies, our study used 3D-MRI images to separate the WM and GM; therefore we believe that our study is more accurate than previous studies. Further separation of the subcortical WM and the cortex with PET spatial resolution seems to be difficult. With respect to pathology, there was a report that indicated that the location of Aβ deposits in the WM is directly beneath the GM, and the distribution of Aβ deposits in the WM corresponds to the orientation of the blood vessels (17). Our study reflects theis pathological change in AD brain using PiB-PET imaging.

In our study, we did not find significant PiB retention among subcortical WM tissues and the centrum semiovale in AD patients. However, there was significantly higher PiB retention in the centrum semiovale than WM in other subcortical areas in the PiB-negative group. We are not aware of any reports that describe this mechanism. We think this mechanism is due to the different binding characteristics of PiB in the centrum semiovale compared with WM in other areas. PiB has been shown to have decreased binding in areas of demyelination (18). WM in the centrum semiovale may be more resistant to demyelination than WM in other areas. These findings need to be explored further and may potentially be clinically useful in the future.

The finding that there is higher PiB retention in the subcortical WM may be helpful in elucidating AD pathogenesis and may help in understanding how WM degeneration occurs in AD. Despite the known importance of WM abnormalities in the pathogenesis of AD, the causes and mechanisms of WM degeneration are still

unknown. It has been reported that increasing cortical hyperphosphorylated tau burden independently predicts the severity of WM hyperintensities. This report suggests that the presence of WM hyperintensities may indicate cortical AD-associated pathology rather than small vessel disease in AD patients (19). Brian and colleagues (20) investigated whether elevated levels of amyloid deposition in PiB-PET and WM hyperintensities in MRI T2-weighted scan is predictive of cognitive impairment. They found that the levels of amyloid deposition, as well as ratings of periventricular WM hyperintensities and deep WM hyperintensities discriminated between cognitively normal and demented individuals. In this study, we did not investigate WM hyperintensities in MRI. There may be a possibility that WM hyperintensities in MRI and amyloid deposition in the subcortical WM have a pathophysiological connection. Whether amyloid deposition occurs earlier in cortices or in subcortical regions is not well known and therefore further investigation is needed.

This study has three limitations. First, there is a patient selection bias. Various categories of non-demented subjective cognitively impaired subjects for the PiB-negative group were included in this retrospective study. We investigated consecutively admitted subjects with different causes of cognitive impairment, because we believe that such a sample is more representative of the actual clinical setting. Second, our study analyzed amyloid deposition with PET images, but was not confirmed by histopathology; thus further histopathological confirmation is needed. Third, we could not completely exclude PiB spillover to the WM from cortex deposition due to the spatial resolution of PET imaging, but our study could more accurately separate WM and cortex deposition by using 3D-MRI data compared with previous studies (2.16). Furthermore, we investigated amyloid deposition in cortical SUVR in both groups and all cortical SUVRs in the AD group were significantly larger than WM SUVRs in AD groups ($P < 0.05$). Although there are specific amyloid depositions in both groups, there is one case that frontal subcortical WM is superior than frontal cortical SUVR. This fact may deny PiB spillover to the subcortical WM from cortex deposition. Unfortunately, there are no reports whether amyloid deposits earlier in cortex or subcortical WM as far as our search. Our study suggested the fact that amyloid deposits in subcortical white matter in AD patients and our study confirmed a previous pathological report that the location of Aβ depositions in the WM was directly beneath the GM (17).

CONCLUSION

We found that in AD brains the PiB uptake in the subcortical WM of frontal, parietal and posterior cingulate regions was significantly larger than in non-AD brains, except in the centrum semiovale WM. These findings may reflect an important pathological feature, even in the WM of AD brain.

REFERENCES

1. **Reitz, C., Brayne. C., and Mayeux, R.** 2011. Epidemiology of Alzheimer disease. Nat Rev Neurol. **7:**137-52.
2. **Braak, H., and Braak, E.** 1995. Staging of Alzheimer's disease-related neurofibrillary changes. Neurobiol Aging. **16:**271-8
3. **Klunk, W.E.** 2011. Amyloid imaging as a biomarker for cerebral beta-amyloidosis and risk prediction for Alzheimer dementia. Neurobiol Aging. **32**:20-36.
4. **Klunk, W.E., Engler, H., Nordberg, A., Wang, Y., Blomqvist, G., Holt, D.P., et al.** 2004. Imaging brain amyloid in Alzheimer's disease with Pittsburgh Compound-B. Ann Neurol. **55:**306-19.
5. **Amlien, I.K., and Fjell, A.M.** 2014. Diffusion tensor imaging of white matter degeneration in Alzheimer's disease and mild cognitive impairment. Neuroscience. **276:**206-15.
6. **Sachdev, P.S., Zhuang, L., Braidy, N., and Wen, W.** 2013. Is Alzheimer's a disease of the white matter? Curr Opin Psychiatry. **26:**244-51.
7. **McKhann, G., Drachman, D., Folstein, M., Katzman, R., Price, D., and Stadlan, E.M.** 1984. Clinical diagnosis of Alzheimer's disease: report of the NINCDS-ADRDA Work Group under the auspices of Department of Health and Human Services Task Force on Alzheimer's Disease. Neurology. **34:**939-44.
8. **Mathis, C.A., Wang, Y., Holt, D.P., Huang, G.F., Debnath, M.L., and Klunk, W.E.** 2003. Synthesis and evaluation of 11C-labeled 6-substituted 2-arylbenzothiazoles as amyloid imaging agents. J Med Chem. **46:**2740-54.
9. **Ishii, K., Soma, T., Kono, A.K., Sofue, K., Miyamoto, N., Yoshikawa, T., et al.** 2007. Comparison of regional brain volume and glucose metabolism between patients with mild dementia with lewy bodies and those with mild Alzheimer's disease. J Nucl Med. **48:**704-11.
10. **Evans, A.C., Janke, A.L., Collins, D.L., and Baillet, S.** 2012. Brain templates and atlases. Neuroimage. **62:**911-22.
11. **Ashburner, J., and Friston, K.J.** 1999. Nonlinear spatial normalization using basis functions. Hum Brain Mapp. **7:**254-66.

12. **Ashburner, J., Neelin, P., Collins, D.L., Evans, A., and Friston, K.** 1997. Incorporating prior knowledge into image registration. Neuroimage. **6:**344-52.
13. **Friston, K.J., Ashburner, J., Frith, C.D., Poline, J.B., Heather, J.D., and Frackowiak, R.S.J.** 1995. Spatial registration and normalization of images. Hum Brain Mapp. **3:**165--89.
14. **Ashburner, J.** 2007. A fast diffeomorphic image registration algorithm. Neuroimage. **38:**95-113.
15. **Matsuda, H., Ohnishi, T., Asada, T., Li, Z.J., Kanetaka, H., Imabayashi, E., et al.** 2003. Correction for partial-volume effects on brain perfusion SPECT in healthy men. J Nucl Med. **44:**1243-52.
16. **Fodero-Tavoletti, M.T., Rowe, C.C., McLean, C.A., Leone, L., Li, Q.X., Masters, C.L., et al.** 2009. Characterization of PiB binding to white matter in Alzheimer disease and other dementias. J Nucl Med. **50:**198-204.
17. **Iwamoto, N., Nishiyama, E., Ohwada, J., and Arai, H.** 1997. Distribution of amyloid deposits in the cerebral white matter of the Alzheimer's disease brain: relationship to blood vessels. Acta Neuropathol. **93:**334-40.
18. **Stankoff, B., Freeman, L., Aigrot, M.S., Chardain, A., Dolle, F., Williams, A., et al.** 2011. Imaging central nervous system myelin by positron emission tomography in multiple sclerosis using (methyl-(1)(1)C)-2-(4'-methylaminophenyl)- 6-hydroxybenzothiazole. Ann Neurol. **69:**673-80.
19. **McAleese, K.E., Firbank, M., Dey, M., Colloby, S.J., Walker, L., Johnson, M., et al.** 2015. Cortical tau load is associated with white matter hyperintensities. Acta Neuropathol Commun. **3:**60-70.
20. **Gordon, B.A., Najmi, S., Hsu, P., Roe, C.M., Morris, J.C., and Benzinger, T.L.** 2015. The effects of white matter hyperintensities and amyloid deposition on Alzheimer dementia. Neuroimage Clin. **8:**246-52.